arXiv:1405.4911v1 [cond-mat.mtrl-sci] 19 May 2014

Fluorine absorption on single and bilayer graphene: Role of sublattice and layer decoupling

Hernán Santos[1,2] **and Luc Henrard**[2]

[1] Departamento de Física Fundamental, Universidad Nacional de Educación a Distancia, Apartado 60141, E-28040 Madrid, Spain

[2] Research Center in Physics of Matter and Radiation (PMR), University of Namur, Rue de Bruxelles 61, B-5000 Namur, Belgium

E-mail: hernan.santos@fisfun.uned.es, luc.henrard@unamur.be

Abstract.

The fluorination of mono- and bi-layer graphene have been studied by means of ab-initio DFT calculations. The stability of CF_x systems are found to depend on both the F coverage and on the position of the F atoms regarding the C sublattices. When F atoms is chemisorbed to C atoms belonging to the same sublattice, low coverage is preferred. Otherwise, large F coverable is more stable (up to C_4F). The difference of charge distribution between the two carbon sublattices explains this finding that is confirmed by the analysis of the diffusion barriers. Binding energy of F on bi-layer systems is also computed slightly smaller than on monolayer and electronic decoupling is observed when only one of the layer is exposed to fluorine.

PACS numbers: 61.48.Gh, 71.15.Mb, 73.22.Pr

Keywords: Graphene, Bilayer Graphene, Fluorine Functionalization, Simulation, Electronic Properties, Binding Energy

Graphene is one of the most promising materials for optical and electronic applications [1]. One of the direction of research to control its electronic properties is the creation of topological defects [2, 3] and the chemical functionalization [4, 5, 6, 7, 8]. A change of the global doping level of electrons or holes could then be obtained together with a modification of the local electronic properties, depending on the type, on the concentration and on the position of the defects [9, 10, 11, 12].

In particular, due to the covalent character of the carbon-fluorine bonds, the F functionalization of graphene is rather easy and large amount of experimental [9, 10, 13, 14, 15, 16, 17, 18, 19] and theoretical [20, 21, 22, 23] works have been reported on the nature of the fluorination of graphene. The CF systems, with a coverage of the two sides of graphene layer, called fluorographane, has demonstrated thermal and chemical stability until 600 K[10] and a bandgap around 3.8 eV[17, 10]. Potential applications in electronic and optoelectronic devices have been proposed[17]. Other F coverage densities modify the bandgap as well as the electronic behavior of the samples[14, 18, 19, 20]. Moreover, fluorination of selective-areas of graphene has been achieved by removing F from graphene by Electron Beam[18] or by local deposition of F by Laser irradiation with Fluoropolymers [19].

Other authors reported a saturated F coverage at 25% (C_4F) over one side of graphene[9, 16]. These results can also be influenced by the number of layers of graphene [16]. A fully fluorinated bilayer graphene has also been predicted to be more stable than pristine bilayer graphene [24] because the sp^3 character of the C-F bonds promotes C-C bonds between layers.

The nature and consequences of the absorption of fluorine on single- and bi-layer graphene have however not been fully investigated. The formation of sp^3 bonds following the F adsorption is, as a first approximation for π-electrons, similar to the presence of vacancies. Both give rise to localized states at or near the Dirac point [12]. The basics of the emergence of these states lies in the presence of two sublattices in graphene [25]. When one p_z orbital is removed in an otherwise perfect lattice, a zero-energy state appears on the other sublattice, damped with the distance [26, 27]. This has also been reported for Hydrogen absorption [28, 29]. The importance of the sublattice symmetry in chemically modified graphene has also been reported for nitrogen substitution [30]. The analysis of the stability, of the chemical bonding and of the electronic properties of fluorinated graphene for different coverage densities and sublattice symmetries is then necessary.

In the present work, we investigate the binding energy (BE) and electronic properties of fluorinated single- and bi-layer graphene by density functional theory (DFT)*ab-initio* calculations. Our results demonstrate that the BE strongly depends on the F coverage density but also on the sublattice of the carbon atoms covalently bonded with the F atoms. Indeed, BE increases for high coverage when carbon of different sublattices are involved in the C-F bonds and BE decreases otherwise. This result is analyzed in terms of sublattice symmetry of the charge distribution associated with a simple defect or adatom. The analysis of the diffusion barriers of F on graphene

reinforces the low probability of same sublattice chemisorption for high F coverage. The electronic properties have also been found to depend on the symmetry of the coverage : fluorinated graphene is an insulator when different sublattice are occupied and metallic when only one sublattice is considered. Furthermore, magnetic behavior is observed only for the less stable configurations, i.e., when only one sublattice is involved. For bilayer graphene, the BE is obtained slightly smaller than for monolayer, in agreement with experimental data [16] and an electronic decoupling between the carbon layers is observed when only one of the two layer is covered with fluorine.

Methods

First principles calculations have been performed using the VASP code with spin polarization [31]. We use the van der Waals functional parameterized by M. Dion *et al.* (vdW-DF) [32], which has been implemented in the code by J. Klimes *et al.* [33]. The factorization proposed in Ref. [34] represents a very substantial efficiency improvement in the evaluation of the exchange-correlation potential and energy, thus enabling first-principles van der Waals calculations for any system accessible to usual GGAs. The results presented below have been performed using by the functional vdW-DF, but we have checked that other van der Waals functionals implemented in the VASP code preserve the main features found employing vdW-DF. Spin polarized calculations normally require a fine sampling of the Brillouin zone, that we performed with a Monkhorst-Pack scheme and the number of point with dependence on the size of the system. For example, 25x25x1 and 5x5x1 k-points have been considered for C_2F (3 atoms) and $C_{50}F$ (51 atoms), respectively. We have verified that the interlayer space in graphite is in agreement with previous calculations [32, 35]. The cut-off energy for plane wave basis set is 500 eV. The structure was relaxed by conjugate gradients optimization until forces are smaller than 0.01 eV/Å. Periodic boundary conditions were applied, so we use large enough supercell parameters (33 Å) in the directions perpendicular to the graphene plane to avoid spurious interactions between adjacent layers.

In order to investigate the stability of the fluorinated coverage, we calculate, from the total energies, the binding energy (BE) per fluorine atom as the difference between the fluorinated graphene (CF_x) and an isolated graphene plus atomic fluorine.

The surface diffusion of F on graphene have been evaluated with the nudged elastic band method (NEB) [36], as implemented in VASP. This method allows to keep the distances between the images along a path constant to first order.

Fluorine coverage of single layer graphene

In order to model the functionalization of graphene with F, we have considered supercells of graphene denoted by nxm, where n and m multiply the unit cell vectors $\vec{a}_1$ and $\vec{a}_2$, respectively (Fig. 1). The number of C atoms per supercell is N =2xnxm. The minimum unit cell of graphene (given by $n = 1$, $m = 1$) has two carbon atoms,

which defined the A and B sublattices. We have considered two important parameters for modelisation of the fluorination of graphene : (i) the density of the coverage, (ii) the position of the F atoms into the supercell (sublattice symmetry and the distances between F atoms). Moreover, except otherwise stated, we have studied systems with the F atoms lying on the same side of the graphene in order to mimick the chemical functionalisation of graphene deposited on a substrate.

We denote the density of coverage by x, in a CF_x (or C_nF_{nx} system). Lower coverages of F atoms is obtained with large supercell, such as $CF_{0.02}$ ($C_{50}F$) generated by a 5x5 supercell. We have considered densities from $x = 0.02$ to $x = 1$. The second important parameter is the position of the F atoms. If only a single F atom is considered for a given supercell, all the F atoms are bonded with C atoms belonging to the same sublattice. The system is called CF_x^{AA}. The effect of the sublattice symmetry can then only be investigated when several F atoms per unit cell are considered and CF_x^{AB} is used for a system with both A and B carbon atoms chemically bonded with F atom.

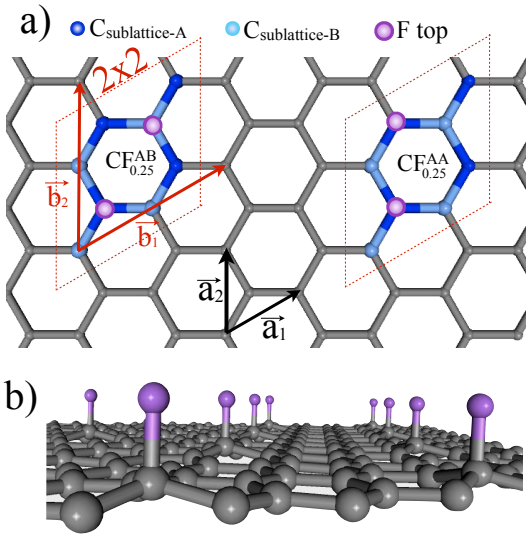

Figure 1. (Color online) a) Schematic representation of a $CF_{0.25}$ (C_8F_2) system in a 2x2 graphene supercell (red dotted line). Light (dark) blue balls are for the carbon atom of the sublattice A (B) and purple balls are for the top F atoms. Left : $CF_{0.25}^{AB}$. Right : $CF_{0.25}^{AA}$. b) 3D representation of C_8F^{AA} in a 2x2 graphene supercell.

The most stable system reported until now is the fluorographane (CF) [9] with a F atom bonded to each C atoms, on both sides of the graphene plane. The BE in the present van der Waals scheme calculations is found to be BE= 2.78 eV. In ref. [37] a BE= 2.86 eV has been calculated by first principles using a different functional (PBE). Note, two F atoms over the same side of graphene plane in a CF system is not stable due to the repulsion between F atoms.

As a second example, we consider C_2F^{AA} with a F atom in a 1x1 supercell with all the F atoms attached to a same sublattice C atom (say, the A sublattice). C_2F^{AA} is the less stable configuration studied in this work with a BE= 0.90 eV. Its counterpart, with the same concentration $x = 0.5$ in the AB configuration ($C_4F_2^{AB}$) in a 2x1 supercell and

F atoms on both sides of the graphene layer to avoid repulsion between first neighbour F atoms has a BE= 2.47 eV. This means a difference of 1.57 eV for the same density.

C_8F_2 is obtained with a 2x2 supercell with 2 F atoms (Fig. 1). When the F atoms are adsorbed on the same side but on different sublattices ($C_8F_2^{AB}$) and with the larger distance between them (equals to the third nearest neighbour), the system is the most stable one-side' fluorinated graphene (BE = 2.27 eV), in agreement with ref [9, 16, 21]. The other possible configuration, $C_8F_2^{AA}$, with the F atoms over the same sublattice, is less favorable by 0.94 eV. The main structural parameter for the stability of graphene-F systems is then the sublattice symmetry.

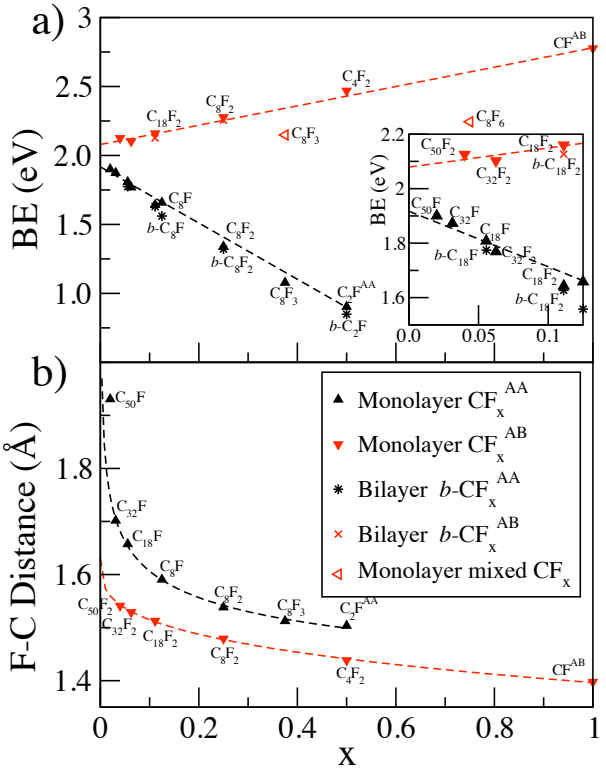

Figure 2. (Color online) Binding energy (BE) (a) and F-C distance (b) of a CF_x as a function of the F concentration x for both sublattice symmetry. Dashed lines are guide for the eyes.

The importance of the sublattice symmetry on the BE is found for all densities of F coverage as shown in Fig. 2a. Note that for the CF_x^{AB} systems, the BE for the most stable position of the two F atoms in the supercell (i.e., the third nearest neighbour) have been reported [38]. We see that the BE of A-B configuration increases almost linearly when the F density rises. This means that, energetically, F atoms tend to form area with high coverage. At the opposite, for the A-A adsorption, the BE decreases almost linearly with the F coverage. For the same coverage, the difference in the BE between the two configurations can be considerable, from 1.57 eV for C_4F_2 to 0.33 eV for $C_{32}F_2$. As expected, for low density, the difference of BE vanishes and the BE is close to 2 eV for both configurations. Therefore, from an experimental point of view,

for low concentration, the F coverage will not depend on the sublattice symmetry, as expected. But when the concentration rises, chemisorption on different sublattices will be favoured.

The importance of the sublattice symmetry is further evidence by the special 'mixed' case of C_8F_3. When the three F atoms are positioned on the same sublattice in a 2x2 supercell, BE=1.08 eV, following the linear behavior found previously. However, when two F atoms are on the A sublattice and the other one in the B sublattice, the BE rise to 2.15 eV but still below the AB curve (Fig. 2a), as a consequence of the 'mixed' sublattice symmetry.

Fluorine functionalization of graphene deforms the planar structure because of the modification of the hybridization of the C-C bounds [21]. Hybridization can be investigated by structural parameters such as the F-C distance and the C-C bond angles (for C involved in the C-F bonds). Angles of 109° (90°) and smaller (larger) F-C distances are expected for perfect sp^3 (sp^2) hybridization. For CF_x^{AB}, distance slightly decreases for larger coverage, from 1.54 Å for $C_{50}F_2^{AB}$ to 1.40 Å for CF^{AB}. At the same time, a small modification of the angles is observed (from 103.5° for $C_8F_2^{AB}$ to 101.5° for $C_{50}F_2^{AB}$) and but no notable change of the charge on the F atoms is observed (0.56 electron). Larger coverage in CF_x^{AB} is then associated with slightly more sp^3 character of the C-F bonds.

For CF_x^{AA}, the C-F distance also decreases with the coverage (Fig. 3b). This is associated with a more pronounced change of the angle from 101.4° (C_2F^{AA}) to 96.3° ($C_{50}F^{AA}$) and of a charge transfer varying from 0.47 electron (C_2F^{AA}) to 0.62 electron ($C_{50}F^{AA}$). For CF_x^{AA} also, larger coverage is associated with more sp^3 character of the C-F bonds. However, at low coverage the C-F bonds is more ionic and the C-C bonds are sp^2. The presence of two kinds of C-F bonds (one ionic associted with sp^2 and one more covalent associated with sp^3 have been observed experimentally by XPS measurement [16].

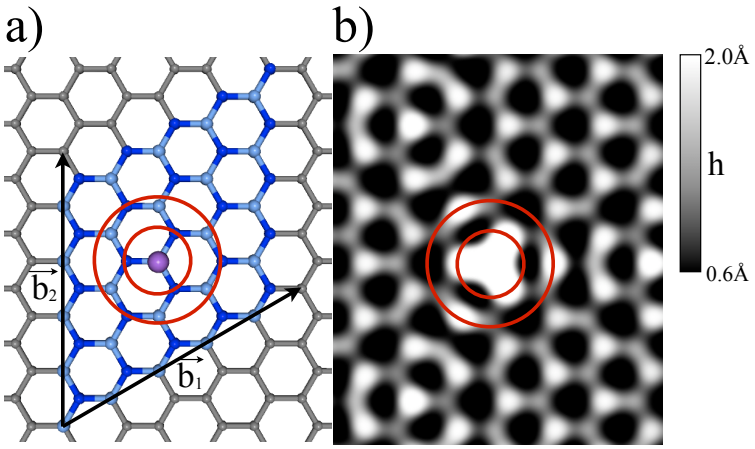

Figure 3. (Color online) a) $C_{50}F$ system. $\vec{b}_1$ and $\vec{b}_2$ indicate the supercell vector in the graphene plane. b) simulated STM image. The inner and the outside red circles indicate first and third neighbour from F-C bond, respectively.

An isolated chemical doping or defect breaks the sublattice symmetry as demonstrated for vacancies [27], nitrogen substitution [30] or H chemisorption [28, 29]. In order to demonstrate this feature for F chemisorption on graphene and interprete the difference observed above for the two systems, we present on Fig. 3 a simulated STM images of $C_{50}F^{AA}$ ($x = 0.02$) in the Tersoff-Hamman approximation for the electronic states between E_F and $E_F + 1eV$. Note that this image has been computed for the 'free' side of the graphene in order to avoid the direct imaging of the F atom. Fig.3 then shows the carbon local electronic density of states near the Fermi level for a $C_{50}F^{AA}$ system. The enhanced electronic density on the B sublattice is clearly evidenced (F atom is on the A sublattice). The formation of a sp^3 bond on one sublattice then induces an increase of the electron density (near the Fermi level) on the other sublattice, as for vacancies. A second electronegative F atom then preferentially form covalent sp^3 bonds with carbon atoms of the other (B) sublattice, presenting an excess of electrons. This effect vanish with the distance between two F atoms because of the screening and smaller distance between F atoms (larger coverage) is favored. If the same (A) sublattice is considered, the low electron density will favor a ionic C-F bonds and sp^2 C-C bonds.

Following this argument, for the second F atom, the first neigbours A-B functionalisation should be more stable. But the F-F repulsion excludes this possibility. We have further checked the role of the F-F repulsion for the $C_8F_2^{AB}$. When the two F atoms are positioned on the same side as first nearest neighbour, the BE is 1.80 eV. But when the F atoms are chemisorbed on different side of the graphene, the BE rises to 2.42 eV per F atom. This large different energy (0.62 eV per F atom) is mainly related to the repulsion between the F atom. This is further proved if we analyze the same $C_8F_2^{AB}$ system but with two F atoms at third nearest neighbour position. In this case, BE=2.27 eV for the F atoms lying on the same side of the graphene and BE = 2.28 eV for the F atoms on both sides of graphene. The small difference of energy in this last case demonstrates the preponderance of the charge distribution on the graphene sublattice for the analysis of the BE.

Diffusion barrier

Beside the total energy calculations, diffusion of F atoms on the graphene surface is influenced by the F coverage. We use the nudged elastic band (NEB) method to evaluate the diffusion barrier of F atoms on graphene. The diffusion barrier of an isolated F on graphene is found to be 356.4 meV for a 2x2 supercell. This very high barrier (more than 10 times the thermal energy) is expected because of the covalent C-F bonds. F atoms are then not mobile on a graphene surface.

The picture changes completely if a F atom is already chemisorbed on graphene. Energy barrier in a 2x2 supercell with 2 F atoms (C_8F_2) is displayed on Fig. 4. As discussed before, the most stable situation is found for a F atom bonded to C atoms of different sublattices but not first neighbours (F1 and F2 positions on fig. 4). To move one F atom from the stable position to the neighbouring A site (path 1 from B

to A on Fig. 4), the F2 atom has to overcome a barrier that is larger than 2 eV and that correspond more or less to the difference of binding energy between the structures. Interestingly, despite the covalent C-F bonding, the reverse path has a barrier of only 47 meV. This process is likely to occurs thermally. The diffusion to the first-neighbour position (path 2) is very unlikely even if the final position is more stable (diffusion barrier 254 meV).

We note here that if the two F atoms are first neighbour, in spite of the repulsion between the two F atom, this configuration is more stable than the A-A configuration and the energy barrier along path 2 (From B to A) in more than 1 eV. However, this situation is very unlikely to occurs because in a deposition process first neighbour positions will be prevent by the F-F repulsion before C-F bonds can be formed.

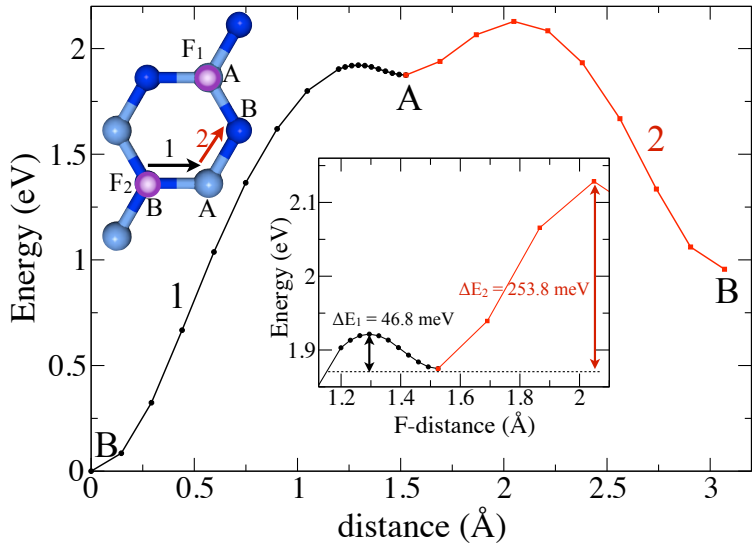

Figure 4. (Color online) Energy barrier in a C_8F_2 system when a F_2 atom moves along the paths 1 (black line) and 2 (red line).

Electronic properties

We now turn to the analysis of the the band structures (BS) of the C-F systems. For single-layer graphene, as for the BE, the electronic behaviour depends strongly on the arrangement of the F atoms into the unit cell. For high F concentration the Dirac cone of the pristine graphene disappears for both F sublattices arrangements (Ref [20] and Fig. 5). For exemple, $C_8F_2^{AA}$ has almost flat bands crosses the Fermi level (Fig. 5a) and the local density of states (not shown) shows, as expected, a localization of the associated wavefunctions on the other (B) sublattice. The system is magnetic with a magnetic moment of $0.799\mu_B$. For the other (more stable) configuration, the $CF_{0.25}^{AB}$ (Fig. 5b), the system is non-magnetic and semiconducting, with a gap of 2.87 eV, in agrement with [20]. For larger coverage, C_2F^{AA} system is metallic and has a magnetic moment of $0.745\mu_B$, while $C_4F_2^{AB}$ is non-magnetic and presents a 1.84 eV gap.

For lower F concentration, the Dirac cone can be visualized and the magnetisation tends to zero. For AA configurations, difference also appears depending of the symmetry of the graphene nxn supercell. As for nitrogen [30], if n is a multiple of three (Fig. 5c for the 3x3 system), no gap is created. In the other case, the Dirac cone is opened at the K point of the Bruillouin Zone (Fig. 5d for the 4x4 system). We also note, the p-doping of the graphene layer (the Dirac energy is above the Fermi energy) associated with the electronegativity of the Fluorine atoms.

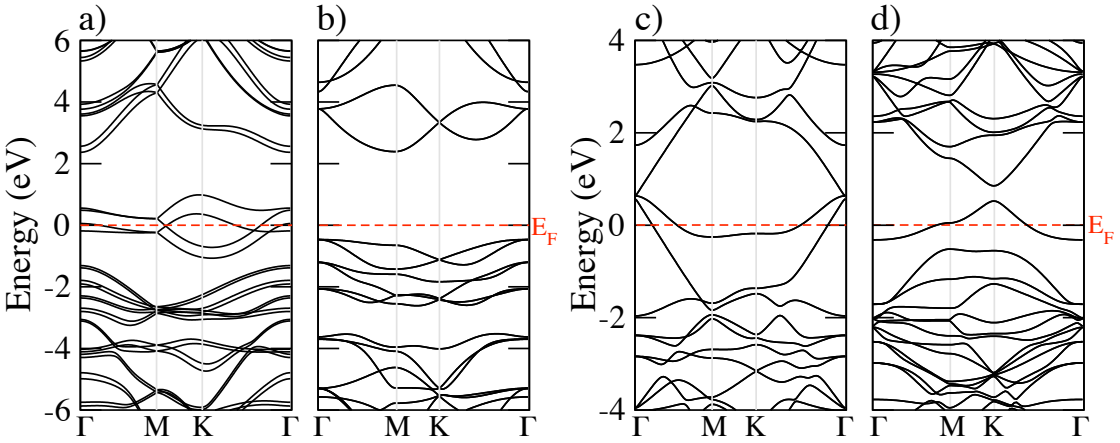

Figure 5. Band structures of a) $C_8F_2^{AA}$, b) $C_8F_2^{AB}$, c) $C_{18}F^{AA}$, and d) $C_{32}F^{AA}$. Red dashed line corresponds the Fermi level (E_F).

Bilayer graphene

For bilayer graphene, denoted as b-C_nF_{nx}, we have only considered the most stable Bernal (AB) stacking and F atoms bonded only to one of the two layers, in order to mimick the chemical functionalisation of graphene lying on a substrate. Because of the Bernal stacking, the symmetry of the sublattice is broken and the two sublattices correspond to inequivalent absortion sites. The different in total energy calculation between a F chemisorbed on the A (carbon atom on the top of a carbon atom of the other layer) and B (carbon atom of the top of the center of an hexagon) sublattices decays with the size of the system, and is in favor of the B sublattice. This difference is however much smaller than the one associated with the lattice assymmetry (9.4, 2.5 and 0.4 meV per F atom for b-C_2F, b-C_8F and b-$C_{18}F$, respectively). Note the difference found in Ref. [24] is 0.3 meV but with a PBE functional and a F coverage for the two sides of bilayer graphene.

The BE for b-CF_x, with F atoms chemisorbed on one of the layers only, follows the trends observed for single-layer graphene (Fig. 2). b-CF_x however exhibits systematically smaller BE than monolayer CF_x. The difference is however very small (0.033 eV for $C_{18}F^{AA}$) and is barely visible on the figure. A fluorination of a bilayer graphene energetically less favorable than for monolayer is on agreement with the recent

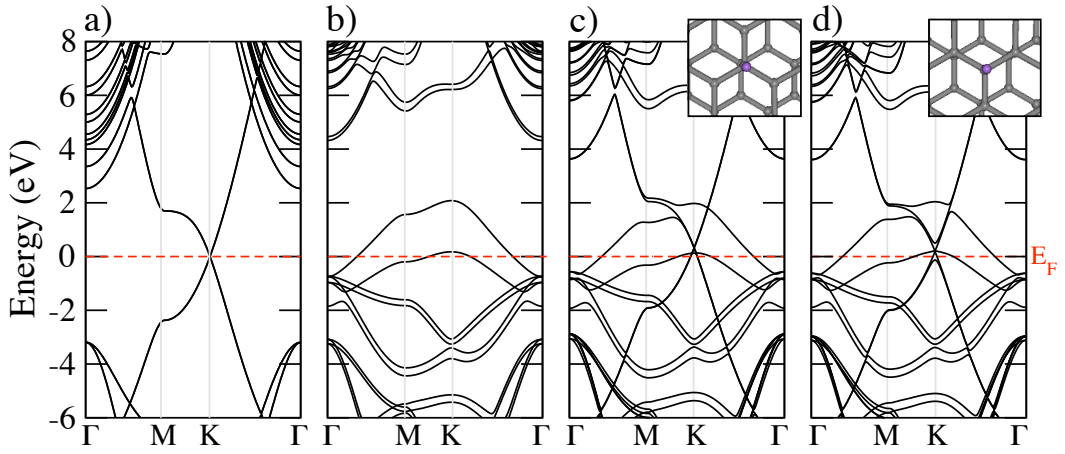

Figure 6. (Color online) Band structure of a) graphene 1x1, b) C_2F^{AA}, c) *b*-C_2F^{AA}, and d) *b*-C_2F^{BB}. Red dashed line corresponds the Fermi level (E_F).

experimental data of Felten *et al.* [16] even if the present order of magnetitude is too small to explain the observations. Note also that the difference between *b*-$C_8F_2^{BB}$ and *b*-$C_8F_2^{AB}$ is of 0.94 eV in favor of the AB case, similar to the diffrence for single layer graphene (Fig. 2).

Charge calculations indicate a weak charge transfer from the pristine layer to the functionalized layer of 0.0043 e per C atom for *b*-C_2F^{AA} system, 0.0029 e per C atom for *b*-C_8F^{AA}.

Fluorination also influences the interlayer interaction energy (ILE) per carbon atom. For example, ILE are found to be 0.016 eV and 0.021 eV for *b*-C_2F^{AA} and *b*-C_2F^{BB}, respectively, compared with 0.050 eV for pristine bi-layer [35]. For more stable $C_8F_2^{AA}$, $C_8F_2^{BB}$ and $C_8F_2^{AB}$ ILE is even smaller (0.015, 0.001 and 0.002 eV, respectively). A decoupling between the graphene layers then occurs due to the fluorination and is correlated with the sp^3 hybridization of one of the layers. A decoupling in bilayer graphene has also been observed [39] and simulated for oxygen chemisorption [40]. At the opposite, a fluorination of both side of bilayer graphene lead to a strong coupling due to the formation of sp^3 bonds between C atoms of different layers [24].

The electronic band structures (BS) of the systems also demonstrate the decoupling between the two layers when one of them is fluorinated. Fig. 6 c and d show the BS of a *b*-C_2F when the F atom is bonded to the A and B sublattices, respectively. For comparison, the BS of pristine graphene single layer (Fig. 6a) and single layer C_2F^{AA} (Fig. 6b) are also presented . The BS of the *b*-C_2F^{AA} system is almost the sum of two isolated systems. The fluorination of one of the layer of bi-layer graphene then results in an electronic decoupling of the two layers and Dirac fermion behavior is recovered on the pristine layer. The Dirac cone is slighly shifted up due to the p-doping mentionned earlier. If we closely look at the Dirac point, the electronic decoupling is better for C_2F^{AA}, as expected from the ILE results. Similar results have been obtained for smaller coverage, with a smaller decoupling as the coverage decreases. (see Suppl. Information).

Nevertheless, for the energetically favourable b-$C_8F_2^{AB}$ the decoupling is still strong.

Summary

In conclusion, the nature of the F functionalization of graphene and bilayer graphene have been addressed. The study by means of van der Waals first-principles calculations demonstrate the sublattice dependence in chemisorption in graphene. The most stable F coverages are obtained when the two sublattices are equally occupied by F atom. Combined with the short range F-F repulsion, the most stable system is C_4F, as observed experimentally [9, 16, 17]. Energy barriers calculations reinforced this conclusion. Bilayer flurorination is slightly less favourable energetically but present an interesting electronic decoupling between graphene layer. This decoupling could be observabled experimentally by STM, Raman [41, 39], transport measurements or ARPES. Chemisorption of top layer bilayer graphene can be a way to (locally) create an electronically single-layer graphene sandwiched between an insulating F functionalized graphene layer and the substrate.

Acknowledgments

The authors thank Thomas Chanier for helpfull advices on NEB calculations and Alexandre Felten usefull discussions on experimental data. This work was supported by Spanish Ministry of Economy and Competitiveness (MINECO) under Grants No. FIS2010-21282-C02-02 and used resources of the "Plateforme Technologique de Calcul Intensif (PTCI)" (http://www.ptci.unamur.be) located at the University of Namur, Belgium, which is supported by the F.R.S.-FNRS under the convention No. 2.4520.11. The PTCI is member of the "Consortium des quipements de Calcul Intensif (CCI)" (http://www.ceci-hpc.be). H. S. acknowledges the F.R.S.-FNRS for a mobility grant and the hospitality of the Department of Physics of the University of Namur.

References

[1] Castro Neto A H, Guinea F, Peres N M R, Novoselov K S and Geim A K 2009 *Rev. Mod. Phys.* **81**(1) 109–162 URL http://link.aps.org/doi/10.1103/RevModPhys.81.109

[2] Nair R R, Tsai I L, Sepioni M, Lehtinen O, Keinonen J, Krasheninnikov A V, Castro Neto A H, Katsnelson M I, Geim A K and Grigorieva I V 2013 *Nat Commun* **4** URL http://dx.doi.org/10.1038/ncomms3010

[3] Huang P Y, Ruiz-Vargas C S, van der Zande A M, Whitney W S, Levendorf M P, Kevek J W, Garg S, Alden J S, Hustedt C J, Zhu Y, Park J, McEuen P L and Muller D A 2011 *Nature* **469** 389–392 URL http://dx.doi.org/10.1038/nature09718

[4] Elias D C, Nair R R, Mohiuddin T M G, Morozov S V, Blake P, Halsall M P, Ferrari A C, Boukhvalov D W, Katsnelson M I, Geim A K and Novoselov K S 2009 *Science* **323** 610–613 (*Preprint* http://www.sciencemag.org/content/323/5914/610.full.pdf) URL http://www.sciencemag.org/content/323/5914/610.abstract

[5] Balog R, Andersen M, Jrgensen B, Sljivancanin Z, Hammer B, Baraldi A, Larciprete R, Hofmann P, Hornekr L and Lizzit S 2013 *ACS Nano* **7** 3823–3832 (*Preprint* http://pubs.acs.org/doi/pdf/10.1021/nn400780x) URL http://pubs.acs.org/doi/abs/10.1021/nn400780x

[6] Shih C J, Wang Q H, Jin Z, Paulus G L C, Blankschtein D, Jarillo-Herrero P and Strano M S 2013 *Nano Letters* **13** 809–817 (*Preprint* http://pubs.acs.org/doi/pdf/10.1021/nl304632e) URL http://pubs.acs.org/doi/abs/10.1021/nl304632e

[7] Zhang H, Bekyarova E, Huang J W, Zhao Z, Bao W, Wang F, Haddon R C and Lau C N 2011 *Nano Letters* **11** 4047–4051 (*Preprint* http://pubs.acs.org/doi/pdf/10.1021/nl200803q) URL http://pubs.acs.org/doi/abs/10.1021/nl200803q

[8] Kumar P V, Bernardi M and Grossman J C 2013 *ACS Nano* **7** 1638–1645 (*Preprint* http://pubs.acs.org/doi/pdf/10.1021/nn305507p) URL http://pubs.acs.org/doi/abs/10.1021/nn305507p

[9] Robinson J T, Burgess J S, Junkermeier C E, Badescu S C, Reinecke T L, Perkins F K, Zalalutdniov M K, Baldwin J W, Culbertson J C, Sheehan P E and Snow E S 2010 *Nano Letters* **10** 3001–3005 (*Preprint* http://pubs.acs.org/doi/pdf/10.1021/nl101437p) URL http://pubs.acs.org/doi/abs/10.1021/nl101437p

[10] Nair R R, Ren W, Jalil R, Riaz I, Kravets V G, Britnell L, Blake P, Schedin F, Mayorov A S, Yuan S, Katsnelson M I, Cheng H M, Strupinski W, Bulusheva L G, Okotrub A V, Grigorieva I V, Grigorenko A N, Novoselov K S and Geim A K 2010 *Small* **6** 2773–2773 ISSN 1613-6829 URL http://dx.doi.org/10.1002/smll.201090086

[11] Lehmann T, Ryndyk D A and Cuniberti G 2013 *Phys. Rev. B* **88**(12) 125420 URL http://link.aps.org/doi/10.1103/PhysRevB.88.125420

[12] Santos H, Soriano D and Palacios J J 2014 *Phys. Rev. B* **89**(19) 195416 URL http://link.aps.org/doi/10.1103/PhysRevB.89.195416

[13] Withers F, Dubois M and Savchenko A K 2010 *Phys. Rev. B* **82**(7) 073403 URL http://link.aps.org/doi/10.1103/PhysRevB.82.073403

[14] Cheng S H, Zou K, Okino F, Gutierrez H R, Gupta A, Shen N, Eklund P C, Sofo J O and Zhu J 2010 *Phys. Rev. B* **81**(20) 205435 URL http://link.aps.org/doi/10.1103/PhysRevB.81.205435

[15] Stine R, Lee W K, Whitener K E, Robinson J T and Sheehan P E 2013 *Nano Letters* **13** 4311–4316 (*Preprint* http://pubs.acs.org/doi/pdf/10.1021/nl4021039) URL http://pubs.acs.org/doi/abs/10.1021/nl4021039

[16] Felten A, Eckmann A, Pireaux J J, Krupke R and Casiraghi C 2013 *Nanotechnology* **24** 355705 URL http://stacks.iop.org/0957-4484/24/i=35/a=355705

[17] Jeon K J, Lee Z, Pollak E, Moreschini L, Bostwick A, Park C M, Mendelsberg R, Radmilovic V, Kostecki R, Richardson T J and Rotenberg E 2011 *ACS Nano* **5** 1042–1046 (*Preprint* http://pubs.acs.org/doi/pdf/10.1021/nn1025274) URL http://pubs.acs.org/doi/abs/10.1021/nn1025274

[18] Withers F, Bointon T H, Dubois M, Russo S and Craciun M F 2011 *Nano Letters* **11** 3912–3916 (*Preprint* http://pubs.acs.org/doi/pdf/10.1021/nl2020697) URL http://pubs.acs.org/doi/abs/10.1021/nl2020697

[19] Lee W H, Suk J W, Chou H, Lee J, Hao Y, Wu Y, Piner R, Akinwande D, Kim K S and Ruoff R S 2012 *Nano Letters* **12** 2374–2378 (*Preprint* http://pubs.acs.org/doi/pdf/10.1021/nl300346j) URL http://pubs.acs.org/doi/abs/10.1021/nl300346j

[20] Liu H Y, Hou Z F, Hu C H, Yang Y and Zhu Z Z 2012 *The Journal of Physical Chemistry C* **116** 18193–18201 (*Preprint* http://pubs.acs.org/doi/pdf/10.1021/jp303279r) URL http://pubs.acs.org/doi/abs/10.1021/jp303279r

[21] Sofo J O, Suarez A M, Usaj G, Cornaglia P S, Hernández-Nieves A D and Balseiro C A 2011 *Phys. Rev. B* **83**(8) 081411 URL http://link.aps.org/doi/10.1103/PhysRevB.83.081411

[22] Şahin H, Topsakal M and Ciraci S 2011 *Phys. Rev. B* **83**(11) 115432 URL http://link.aps.org/doi/10.1103/PhysRevB.83.115432

[23] Wei W and Jacob T 2013 *Phys. Rev. B* **87**(11) 115431 URL http://link.aps.org/doi/10.1103/

PhysRevB.87.115431

[24] Sivek J, Leenaerts O, Partoens B and Peeters F M 2012 *The Journal of Physical Chemistry C* **116** 19240–19245 (*Preprint* http://pubs.acs.org/doi/pdf/10.1021/jp3027012) URL http://pubs.acs.org/doi/abs/10.1021/jp3027012

[25] Inui M, Trugman S A and Abrahams E 1994 *Phys. Rev. B* **49** 3190–3196

[26] Liang S Z and Sofo J O 2012 *Phys. Rev. Lett.* **109**(25) 256601 URL http://link.aps.org/doi/10.1103/PhysRevLett.109.256601

[27] Ducastelle F 2013 *Physical Review B* **88** 075413 (*Preprint* http://journals.aps.org/prb/abstract/10.1103/PhysRevB.88.075413) URL http://journals.aps.org/prb/abstract/10.1103/PhysRevB.88.075413

[28] Duplock E J, Scheffler M and Lindan P J D 2004 *Phys. Rev. Lett.* **92**(22) 225502 URL http://link.aps.org/doi/10.1103/PhysRevLett.92.225502

[29] Soriano D, Leconte N, Ordejón P, Charlier J C, Palacios J J and Roche S 2011 *Phys. Rev. Lett.* **107**(1) 016602 URL http://link.aps.org/doi/10.1103/PhysRevLett.107.016602

[30] Lambin P, Amara H, Ducastelle F and Henrard L 2012 *Phys. Rev. B* **86**(4) 045448 URL http://link.aps.org/doi/10.1103/PhysRevB.86.045448

[31] Kresse G and Furthmüller J 1996 *Phys. Rev. B* **54**(16) 11169–11186 URL http://link.aps.org/doi/10.1103/PhysRevB.54.11169

[32] Dion M, Rydberg H, Schröder E, Langreth D C and Lundqvist B I 2004 *Phys. Rev. Lett.* **92**(24) 246401 URL http://link.aps.org/doi/10.1103/PhysRevLett.92.246401

[33] Klimeš J c v, Bowler D R and Michaelides A 2011 *Phys. Rev. B* **83**(19) 195131 URL http://link.aps.org/doi/10.1103/PhysRevB.83.195131

[34] Román-Pérez G and Soler J M 2009 *Phys. Rev. Lett.* **103**(9) 096102 URL http://link.aps.org/doi/10.1103/PhysRevLett.103.096102

[35] Santos H, Ayuela A, Chico L and Artacho E 2012 *Phys. Rev. B* **85**(24) 245430 URL http://link.aps.org/doi/10.1103/PhysRevB.85.245430

[36] Mills G, Jnsson H and Schenter G K 1995 *Surface Science* **324** 305 – 337 ISSN 0039-6028 URL http://www.sciencedirect.com/science/article/pii/0039602894007314

[37] Leenaerts O, Peelaers H, Hernández-Nieves A D, Partoens B and Peeters F M 2010 *Phys. Rev. B* **82**(19) 195436 URL http://link.aps.org/doi/10.1103/PhysRevB.82.195436

[38] For $C_4F_2^{AB}$, $C_8F_6^{AB}$ and CF^{AB}, F atoms are on both side of the graphene. No configuration with F atoms on the same side of the layer do exit without first neighbour position.

[39] Felten A, Flavel B S, Britnell L, Eckmann A, Louette P, Pireaux J J, Hirtz M, Krupke R and Casiraghi C 2013 *Small* **9** 631–639 ISSN 1613-6829 URL http://dx.doi.org/10.1002/smll.201202214

[40] Nourbakhsh A, Cantoro M, Klekachev A V, Pourtois G, Vosch T, Hofkens J, van der Veen M H, Heyns M M, De Gendt S and Sels B F 2011 *The Journal of Physical Chemistry C* **115** 16619–16624 (*Preprint* http://pubs.acs.org/doi/pdf/10.1021/jp203010z) URL http://pubs.acs.org/doi/abs/10.1021/jp203010z

[41] Chacón-Torres J C, Wirtz L and Pichler T 2013 *ACS Nano* **7** 9249–9259 (*Preprint* http://pubs.acs.org/doi/pdf/10.1021/nn403885k) URL http://pubs.acs.org/doi/abs/10.1021/nn403885k

Supporting information: Fluorine absorption on single and bilayer graphene: Role of sublattice and layer decoupling

Hernán Santos[1,2] and Luc Henrard[2]

[1] Departamento de Física Fundamental, Universidad Nacional de Educación a Distancia, Apartado 60141, E-28040 Madrid, Spain
[2] Research Center in Physics of Matter and Radiation (PMR), University of Namur, Rue de Bruxelles 61, B-5000 Namur, Belgium

E-mail: hernan.santos@fisfun.uned.es, luc.henrard@unamur.be

PACS numbers: 61.48.Gh, 71.15.Mb, 73.22.Pr

Keywords: Graphene, Bilayer Graphene, Fluorine Functionalization, Simulation, Electronic Properties, Binding Energy

Supporting information: Fluorine absorption on single and bilayer graphene: Role of sublattice and layer

In this supporting information we provide additionnal band structures of fluorinated bi-layer graphene as a further illustration of the electronic decoupling that occurs when the F is chemisorbed on one of the two layers (Figs. 7, 8, 9, 10, and 11).

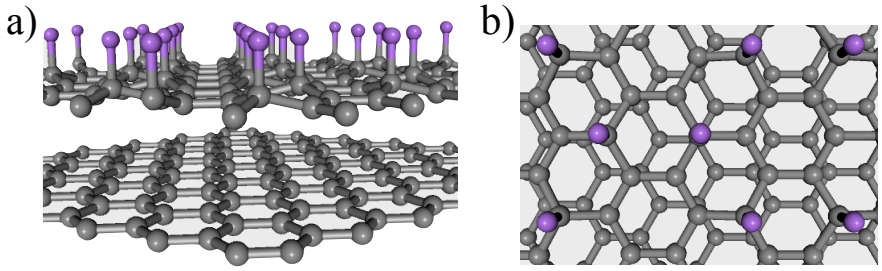

Figure 7. (Color online) 3D view of a bilayer graphene which is coveraged on the one side of one of the layers by F. The figures correspond to b-$C_8F_2^{AB}$ in a a) lateral and b) planar view.

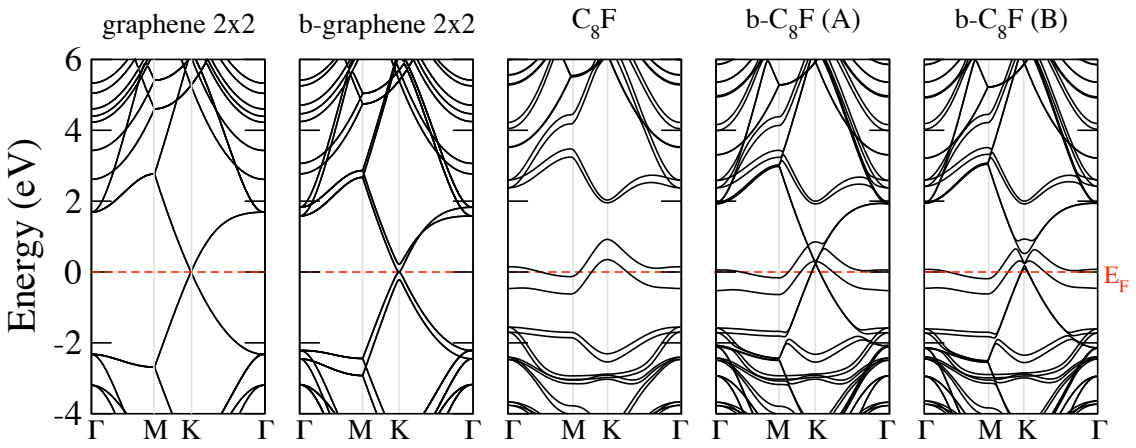

Figure 8. (Color online) Band structure of a) graphene 2x2, b) bilayer graphene 2x2, c) C_8F^{AA}, d) b-C_8F^{AA}, and e) b-C_8F^{BB}. Red dashed line indicates the Fermi level (E_F).

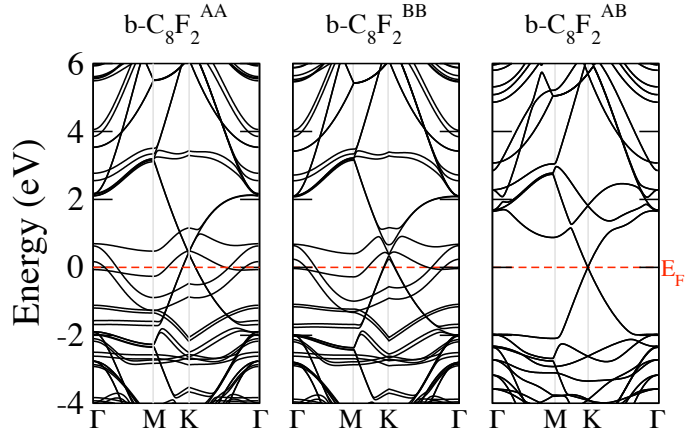

Figure 9. (Color online) Band structure of a) b-$C_8F_2^{AA}$, d) b-$C_8F_2^{BB}$, and e) b-$C_8F_2^{AB}$. Red dashed line indicates the Fermi level (E_F).

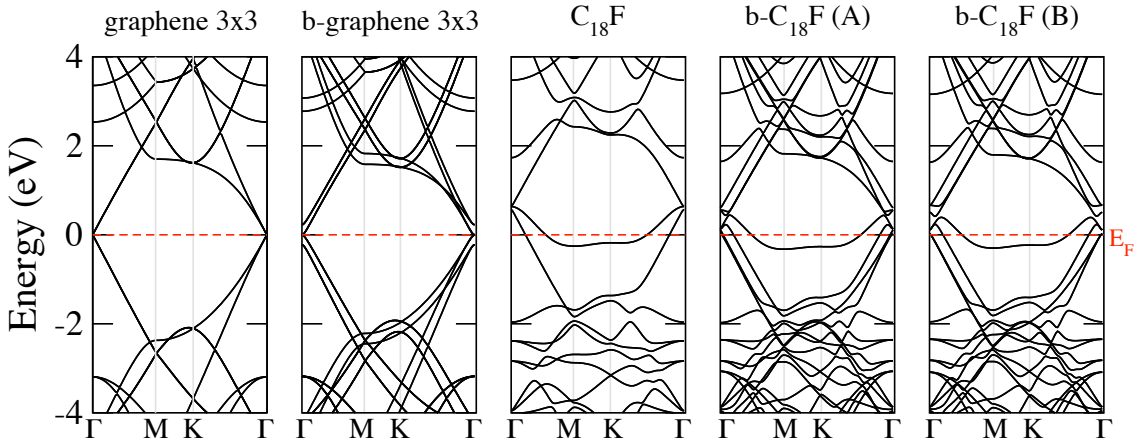

Figure 10. (Color online) Band structure of a) graphene 3x3, b) bilayer graphene 3x3, c) $C_{18}F^{AA}$, d) b-$C_{18}F^{AA}$, and e) b-$C_{18}F^{BB}$. Red dashed line indicates the Fermi level (E_F).

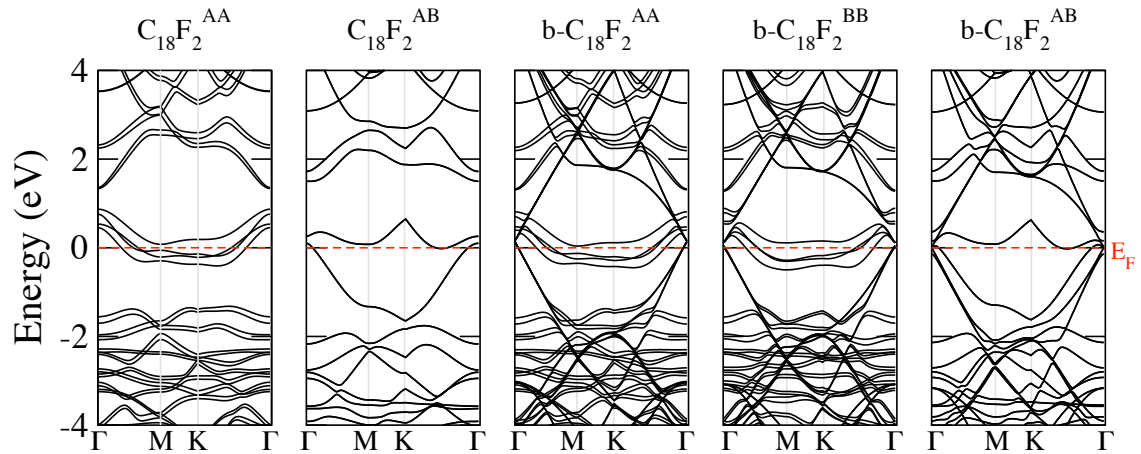

Figure 11. (Color online) Band structure of a) $C_{18}F_2^{AA}$, b) $C_{18}F_2^{AB}$, c) b-$C_{18}F_2^{AA}$, d) b-$C_{18}F_2^{BB}$, and e) b-$C_{18}F_2^{AB}$. Red dashed line indicates the Fermi level (E_F).